CrossMark

ORIGINAL ARTICLE

Blindness alters the microstructure of the ventral but not the dorsal visual stream

Nina L. Reislev[1,2] · Ron Kupers[2] · Hartwig R. Siebner[1,3] · Maurice Ptito[1,2,4] ·
Tim B. Dyrby[1]

Abstract Visual deprivation from birth leads to reorganisation of the brain through cross-modal plasticity. Although there is a general agreement that the primary afferent visual pathways are altered in congenitally blind individuals, our knowledge about microstructural changes within the higher-order visual streams, and how this is affected by onset of blindness, remains scant. We used diffusion tensor imaging and tractography to investigate microstructural features in the dorsal (superior longitudinal fasciculus) and ventral (inferior longitudinal and inferior fronto-occipital fasciculi) visual pathways in 12 congenitally blind, 15 late blind and 15 normal sighted controls. We also studied six prematurely born individuals with normal vision to control for the effects of prematurity on brain connectivity. Our data revealed a reduction in fractional anisotropy in the ventral but not the dorsal visual stream for both congenitally and late blind individuals. Prematurely born individuals, with normal vision, did not differ from normal sighted controls, born at term. Our data suggest that although the visual streams are structurally developing without normal visual input from the eyes, blindness selectively affects the microstructure of the ventral visual stream regardless of the time of onset. We suggest that the decreased fractional anisotropy of the ventral stream in the two groups of blind subjects is the combined result of both degenerative and cross-modal compensatory processes, affecting normal white matter development.

Keywords Tractography · White matter microstructure · Congenital and late blindness · Plasticity · Ventral and dorsal visual pathway

✉ Nina L. Reislev
ninar@drcmr.dk

1 Danish Research Centre for Magnetic Resonance, Section 714, Centre for Functional and Diagnostic Imaging and Research, Copenhagen University Hospital Hvidovre, Kettegaard Allé 30, 2650 Hvidovre, Denmark

2 BRAINlab, Department of Neuroscience and Pharmacology, Faculty of Health & Medical Sciences, University of Copenhagen, Copenhagen, Denmark

3 Department of Neurology, Copenhagen University Hospital Bispebjerg, Copenhagen, Denmark

4 School of Optometry, Université de Montréal, Montreal, QC, Canada

Introduction

It is now well established that despite a large atrophy of the primary visual retinofugal system (Shimony et al. 2006; Noppeney 2007; Yu et al. 2007; Ptito et al. 2008; Shu et al. 2009), the primary visual cortex and its efferent streams are able to process non-visual information conveyed by the senses of touch, audition or smell. Indeed, results of many studies concur that congenitally blind individuals are better at processing auditory, tactile and olfactory information, and thereby recruit their occipital cortex (Kupers and Ptito 2011; Kupers et al. 2011a, b). It has also been shown that the occipital cortex of congenitally blind individuals is thicker than in normally sighted individuals, possibly due to the lack of experience-dependent pruning of synapses in the visual cortex (Park et al. 2009; Jiang et al. 2009), and that this change in cortical thickness correlates with improved performance on, e.g. auditory tasks (Voss and Zatorre 2012). Hence, the visual cortex is recruited by a

wide variety of auditory, tactile, olfactory, and cognitive tasks (Kupers et al. 2011b).

Studies from several research groups have shown that congenitally blind individuals can resolve tactile and auditory forms of motion or shape discrimination tasks and, by doing so, recruit the dorsal and ventral visual pathways, respectively (Amedi et al. 2001, 2002; Pietrini et al. 2004; Poirier et al. 2006; Ricciardi et al. 2007; Ptito et al. 2009, 2012; Renier et al. 2009; Matteau et al. 2010; Collignon et al. 2013; Strnad et al. 2013). Although this suggests that the two visual streams are functionally still intact, it is unknown to what extent the long association fibre bundles that underlie these two cortical systems (Ungerleider and Mishkin 1982) are structurally affected by visual deprivation at birth or later in life. In normally sighted individuals, the ventral and dorsal pathways are involved in object recognition and visuo-spatial functions, classically referred to as the "what" and "where" streams, respectively. The ventral stream comprises the occipito-temporal projections from V1 to inferior temporal cortex, with the inferior longitudinal fasciculus (ILF) and the inferior fronto-occipital fasciculus (IFOF) as its main constituents (Kravitz et al. 2013). The dorsal stream, on the other hand, comprises the long bidirectional occipito-parietal-frontal projections between the occipital and the prefrontal cortices via the posterior parietal cortex. The superior longitudinal fasciculus (SLF) is one of the principal fibre bundles of the dorsal stream (Ffytche et al. 2010; Kravitz et al. 2011).

As stated above, previous studies have shown that the primary visual cortex undergoes substantial atrophy in congenitally blind individuals (Noppeney et al. 2005; Ptito et al. 2008). In addition, white matter alterations occur, such as a decrease in total white matter volume (Noppeney et al. 2005; Ptito et al. 2008), and a decreased fractional anisotropy (FA) of the optic radiations and the occipito-temporal pathways (Shimony et al. 2006; Bridge et al. 2009; Shu et al. 2009). Notwithstanding, the primary visual cortex, as well as the dorsal and ventral visual streams, remains functionally active in congenitally blind individuals (Kupers et al. 2011b). The purpose of this study was to examine to what extent congenital and late-onset blindness affects the microstructural features of the secondary visual pathways of the dorsal and ventral streams, the SLF and the ILF and IFOF, respectively. Previous studies have shown larger structural differences in congenital compared to late-onset blindness (Schoth et al. 2006; Li et al. 2013), possibly due to a larger inter-individual variance in the late-onset blind group. However, early evidence using cytochrome oxidase suggests that even partial loss of sight in one eye induces plastic changes in the ocular dominance columns in human primary visual cortex (Horton and Hedley-Whyte 1984) and the degeneration of parvocellular ganglion cells

in age-related macular degeneration (Clarke 1994). We, therefore, hypothesised that late-onset blindness will also induce structural differences in the visual streams, but that the microstructural alterations will be more pronounced in the congenitally compared to the late blind participants. To this end, we used DTI and tractography based on diffusion-weighted MR images (DWI).

Materials and methods

Subjects

We included 12 congenitally blind (mean age 42 ± 13 years), 15 late blind (mean age 52 ± 15 years) and 15 normal sighted control subjects (mean age 46 ± 13 years). Although groups were matched for gender, age, education and handedness, the late blind group had a tendency to be older compared to the two other groups. We, therefore, included age as a possible confounding factor.

The inclusion criteria for blind subjects were constrained to blindness caused by pathology of peripheral origin. Mean onset of blindness in the late blind group was 17 ± 9 years. Table 1 summarises information about participants' age, blindness type, cause and duration, and Braille reading speed. To control for purported effects of preterm birth on brain connectivity, we also included a group of six subjects born 6–12 weeks prematurely (mean age 28 ± 6 years) but with normal vision, and with no known sequelae related to their preterm birth. All participants gave oral and written consent prior to data acquisition, according to the declaration of Helsinki. The ethics committee for the city of Copenhagen and Frederiksberg approved the experimental procedures [Denmark; ethics protocol number (KF) 01 328 723].

Image acquisition

Data acquisition was performed on a 3.0 T Siemens Verio scanner with a 32-channel head coil (Siemens, Erlangen, Germany). A set of whole-brain DWIs were acquired in 61 non-collinear directions with a b value of $b = 1500$ s/mm^2 and 10 non-diffusion-weighted images ($b = 0$ s/mm^2), using the twice refocused spin echo sequence (TE = 89 ms, TR = 11,440 ms, 61 axial slices, isotropic 2.3 mm^3 voxels, and Grappa = 2, with 24 reference lines, scan time = 14 min) (Reese et al. 2003). The phase-encoding direction was set to posterior–anterior to displace chemical shift artefacts from the occipital to the frontal lobe. We also acquired a field map using a double gradient echo sequence (TR = 479 ms, TE1 = 4.92 ms, TE2 = 7.38 ms, isotropic 3 mm^3 voxels).

Table 1 Demographic information and aetiology of the blind subjects

Sex	Age	Blindness				Braille (wpm)
		Cause	Years	BDI	Eyes	
Late blind						
M	66	Glaucoma	56	0.85	No	100
M	64	Retinitis pigmentosa	50	0.78	Yes	63
F	51	Retinal detachment	19	0.37	Yes	98
F	59	Iris infection, cataract	36	0.61	No	16
F	44	Retinal detachment	37	0.84	Yes	75
F	60	Retinal detachment	29	0.48	Yes	34
M	78	Retinal detachment	18	0.23	No	–
M	57	Glaucoma, cataract, retinal detachment	40	0.70	No	51
F	40	Retinoblastoma	38	0.95	No	167
F	36	Glaucoma	28	0.78	No	90
M	74	Eye trauma	60	0.81	No	64
M	44	Retinoschisis	35	0.80	Yes	68
F	25	Glaucoma, cataract, retinal detachment	6	0.24	Yes	–
M	43	Retinoblastoma	41	0.95	No	202
F	39	Retinal detachment	21	0.54	No	13
Congenitally blind						
M	59	ROP	59		Yes	130
M	50	ROP	50		Yes	75
F	37	ROP	37		Yes	100
F	63	ROP, glaucoma	63		No	124
M	37	Unknown	37		Yes	104
M	44	Retinoblastoma	44		No	158
M	51	ROP	51		Yes	75
F	29	ROP	29		Yes	90
F	28	ROP	28		Yes	115
M	59	ROP	59		Yes	147
F	25	ROP	25		Yes	118
M	27	ROP	27		Yes	94

ROP retinopathy of prematurity, *M* male, *F* female, *BDI* blindness duration index, *Eyes* own eyes kept—yes/no, *Braille wpm* braille reading speed in words per minute

Data processing and analyses

Post-processing of the DWIs

We established a pipeline for the processing of the raw DWIs based on existing and in-house developed software in MATLAB R2012a (The mathWorks, Inc., Natick, MA, USA) and SPM 8 (Wellcome Trust Centre for Neuroimaging, UCL, London, UK). Geometric distortions due to susceptibility artefacts were minimised with the application of a voxel displacement map (VDM) estimated from the acquired field map and using the field map toolbox of SPM8 (Jezzard and Balaban 1995). The VDM was coregistered and resliced to DWI resolution. To reduce motion and eddy current-induced distortions, a full affine transformation was calculated of the DWI volumes to mean of the b0-images, using normalised mutual information. The VDM and the transformation were applied to the DWIs, and the images were co-registered to the MNI template by reslicing to 2 mm³ isotropic resolution using 3rd-order B-spline interpolation. No normalisation was performed at this stage. Finally, the orientation of the 61 non-collinear directions was reoriented similarly to the orientation introduced by the applied transformations. We fitted the diffusion tensor model (Basser et al. 1994) to the corrected DWIs, using a weighted linear model estimation implemented in ExploreDTI v. 4.8.2 (Leemans et al. 2009). Then, we derived voxel-wise DTI indices of regional diffusion such as fractional anisotropy (FA), mean diffusivity (MD) as well as radial and axial diffusivity to obtain a comprehensive description of the underlying tissue microstructure (Wheeler-Kingshott and Cercignani 2009).

The FA value describes the shape of the diffusion tensor, while mean diffusivity is a measure that reflects the mean diffusion within the tensor. Radial and axial diffusivity refers to diffusion transversal and longitudinal to the orientation of the tensor.

Tractography

We performed whole-brain deterministic tractography in ExploreDTI, using constrained spherical deconvolution as multi-fibre reconstruction (Jeurissen et al. 2011; Tournier et al. 2011). Tractography was done by emitting one streamline from each voxel, with the following tracking parameters: seed point in each voxel, streamline angle threshold 45°, and length of tract between 50 and 250 mm.

Fibre tract extraction

After calculation of whole-brain tractography, we manually extracted the fibre tracts of interest (ILF, IFOF, and SLF) in both hemispheres in each individual. Based on a number of normal sighted subjects, we set up a protocol for consistent and reproducible fibre tract extraction across individuals, based on the anatomical course of the tract through the brain, and on previous descriptions (Wakana et al. 2003, 2007; Catani et al. 2003; Jellison et al. 2004; Schmahmann et al. 2007; Lawes et al. 2008; Catani and Thiebaut de Schotten 2008; Martino et al. 2010; Thiebaut de Schotten et al. 2011a, b). The tracts were extracted using the "AND" and "NOT" operation drawing tools in ExploreDTI based on the primary diffusion direction colour-encoded FA-map. The ILF was extracted using two "AND" gates that were drawn on coronal sections. The first "AND" gate was placed around the anterior temporal lobe, after the splitting between ILF and IFOF, where the tract enters the external capsule, whereas the second was placed just posterior to the end of the posterior part of the corpus callosum (Fig. 1a). This procedure ensures that only fibres connecting the occipital lobe with the anterior temporal pole were assigned to the ILF, hence excluding other occipital fibres such as the optic radiation. The IFOF was divided into a posterior segment (IFOF1), running from the occipital to the temporal and parietal lobes, and an anterior segment (IFOF2), running from the temporal and parietal to the frontal lobe. This procedure was adopted for the extraction of two homogenous areas of white matter belonging to the IFOF (IFOF1 and IFOF2). The IFOF segments were extracted using three "AND" gates as shown in Fig. 1b. For the anterior segment, the first "AND" gate was placed in a coronal slice anterior to the genu of the corpus callosum and

included all the frontal projections. The second "AND" gate was placed in a coronal slice at the level of the anterior commissure, whereas the third one was placed in a coronal slice just posterior to the downward bend of the uncinate fasciculus. For the extraction of the posterior segment of the IFOF, we reused the second and third "AND" gates of the anterior IFOF portion. Additionally, to circumscribe precisely the occipital fibres of the IFOF1 segment, we reused the second "AND" gate of the ILF fibre extraction as the first IFOF1 "AND" gate (Fig. 1b).

We extracted and analysed the SLF as one single bundle using two "AND" gates (see Fig. 1c) and one "NOT" gate. The first "AND" gate was positioned on a coronal slice at the level of the anterior commissure, whereas the second one was placed at the posterior commissure. The "NOT" gate was placed on an axial slice at the level of the pars triangularis of the inferior frontal gyrus to exclude the arcuate temporal fibres.

Tract volume and tract density measures

To complement the DTI-based microstructural measures, we quantified tract-related group differences using tract volume and tract density measures derived from tractography. It should be noted that these measures are based on streamlines from tractography and, therefore, cannot be directly linked to the true axonal density or fibre tract volume and the latter due to partial volume effects (PVE) (Vos et al. 2011). First, we generated a visitation map for each tract by counting the number of streamlines that have visited or projected through a voxel. The visitation map was then thresholded for a minimal number of hit-counts (min threshold = 1), and binarised into a tract mask. The tract volume is defined as the sum of all voxels within the tract mask, and the tract density as the sum of all visitations within the tract mask divided by the tract volume. Increasing the threshold of hit-counts induces a reduction in the tract volume, as the tract mask will only include the most frequently visited voxels. The end result then represents the core part(s) of the tract.

Controlling for spreading and fanning effects

The diffusion tensor indices are not only sensitive to geometrical features and axonal density but also to macrostructural effects as spreading and fanning of fibres (Zhang et al. 2011). To minimise contamination by the latter, we adopted the following procedures in the statistical analysis. First, we identified a region-of-interest (ROI) where streamlines from tractography visually appeared both highly aligned and dense, as illustrated in Fig. 1d–f. For both hemispheres, we identified the ROIs in all tracts of

Fig. 1 ROI placements for the three tracts: ILF (**a**, **d**), IFOF (**b**, **e**) and SLF (**c**, **f**). The *top panel* shows an example of each of the tracts in a normal sighted subject with the "AND" gates drawn in *white*, overlaid on a direction colour-coded sagittal slice of an FA-map. The *lower panel* shows the segmented tract ROIs based on the "AND" and "NOT" gates
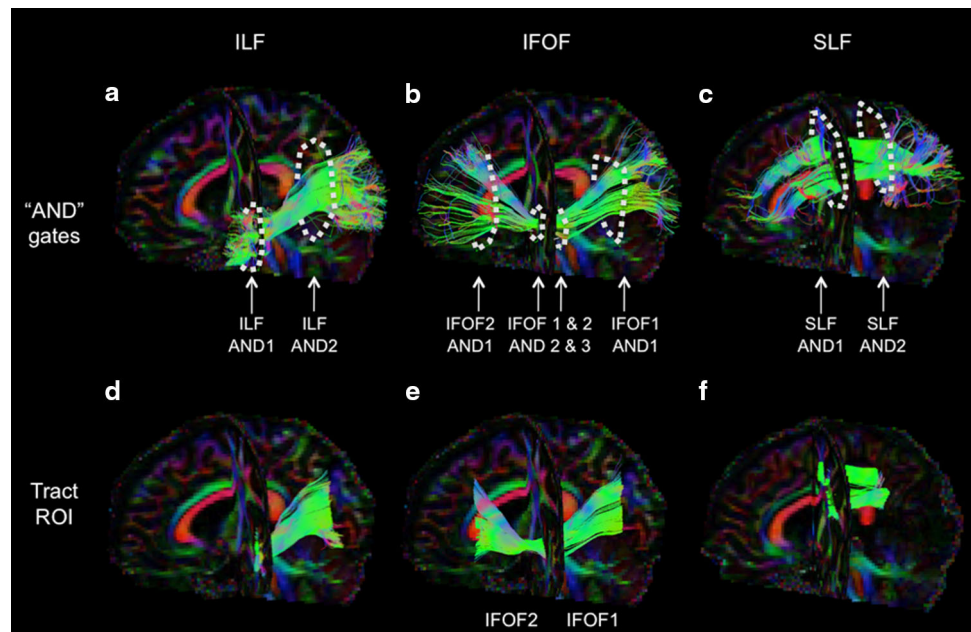
interest, and extracted them using the tract-splitting tool in ExploreDTI. Secondly, we only included voxels in the ROI analysis that were minimally affected by spreading and fanning fibre effects. For this, we used the criteria of high tensor linearity, defined as FA >0.2 and Westins linearity index (WL) >0.1 (Westin et al. 2002). This approach was adopted to perform the DTI analyses within a well-defined ROI, focusing on the microstructural properties within the ventral and dorsal visual streams, and minimising macrostructural effects of the tracts (Vos et al. 2012; Jespersen et al. 2013, 2014; Lasič et al. 2014).

Statistics

We used SPSS Statistics v. 20.0.0 (IBM Corp., Armonk, NY, USA) and MATLAB for statistical analysis. Prior to the statistical analyses, we examined tract volume, tract density, and DTI indices for the assumption of identical distribution with equal variance. We used the Kolmogorov–Smirnov test for examining normality, and the Levene statistics for testing equal variance across groups. Group statistics based on the tract measures of volume and density were performed for each of the tracts of interest. Due to violation of the assumption of normality, we used a non-parametric Kruskal–Wallis ANOVA to assess group-related differences. Tract volume and tract density were examined as a function of the streamline hit-count threshold. A threshold of 1 corresponds to the whole tract, whereas higher thresholds examine potential differences of the tract core parts.

For the ROI analyses, the group statistics investigated the mean and standard deviation of the DTI indices, such as FA and MD as well as radial and axial diffusivity. To test

the hypothesis of alterations in the fibre tracts of congenitally and late blind compared to sighted control subjects, we performed a one-way ANOVA under the null hypothesis of equal means between the three groups, with a rejection criterion at $p < 0.01$. Participants' age and ROI size were included as confounding variables. We used Tukey's test for multiple comparisons to assess significant differences between pairs of means, corrected for the experiment-wise error at the level $\alpha = 0.05$. We performed the same tests for all the tracts and ROIs in each hemisphere. Due to the smaller number of subjects in the preterm control group, we used the non-parametric Kruskal–Wallis ANOVA to test for differences in DTI indices in comparison to blind and normal sighted controls.

We calculated a "blindness duration index" (BDI) defined as years of blindness with respect to the subject's age because this relationship can hold important information on experience-dependent plasticity in the late blind group. The BDI can vary from 0 to 1, with high and low values corresponding to early and late-onset blindness, respectively. We performed a linear regression analysis to assess the relationship between years of blindness, with BDI as explanatory variable, and microstructural tract features, as indexed by FA.
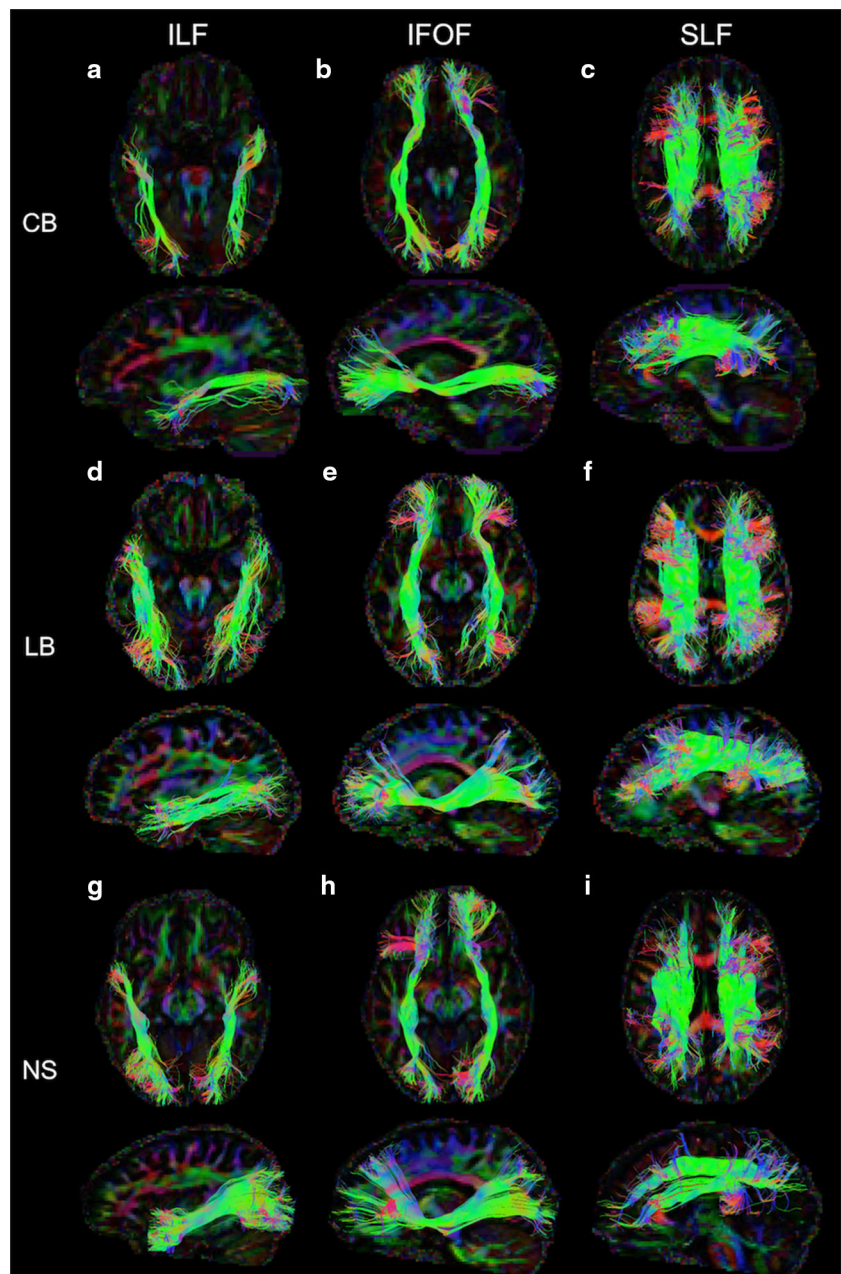
Results

We generally succeeded in fully extracting the three tracts of interest in all groups. The tracts were most consistent along their mid part, and especially the IFOF was ending with spreading and fanning fibres in the frontal lobe.

White matter fibre pathways

Figure 2 shows an example of each of the three extracted association fibre bundles for a typical normal sighted control as well as a late and congenitally blind participant. Visual inspection suggests that the pathway and projection sites are similar in blind and control subjects. The tractography results seem to suggest that the ILF and IFOF project more directly to the visual cortex (Fig. 2g, h) compared to the SLF (Fig. 2i). The ILF also appears less dense in the congenitally blind subject. Visual inspection

further revealed more variability in tract shape and density in the blind subjects, especially in the IFOF and ILF. No de visu differences could be observed in the SLF of blind and sighted participants. Moreover, we did not find significant group differences in whole tract volume or tract density for any of the tracts. Although we did not find a significant group difference at higher hit-count thresholds, we observed a tendency towards lower core tract density of the ILF in the congenitally blind compared to sighted control subjects. No group differences for the SLF were found at any threshold (Supplementary Figure 1).

Fig. 2 Streamline tractography of the extracted fibre tracts of interest in a normal sighted (*NS*), late blind (*LB*) and congenitally blind (*CB*) subject, overlaid on an axial and sagittal direction colour-coded FA-map. The colours of the tracts represent the direction of the first eigenvector, with *green* representing the anterior–posterior direction dominating the long association fibre bundles. The *red* and *blue* colours are most prominent as tract branching and tract termination into the cortex. Visual inspection suggests that some of the fibre tracts, especially the ILF, are less dense in the congenitally blind subject. No obvious group differences are apparent in the SLF

White matter microstructural features

Table 2 summarises the ANOVA results for tract-specific microstructural features in each ROI based on DTI indices. We observed significant group differences ($p < 0.01$) in mean FA and radial diffusivity, but not in MD and axial diffusivity, bilaterally in the ventral pathways (ILF and IFOF1). Figure 3 shows mean FA values for all ROIs. As can be seen, FA values of the ILF and IFOF1 are significantly lower in both groups of blind subjects compared to sighted controls. In contrast, we did not detect between-group differences in FA or diffusivity in the anterior part of the inferior fronto-occipital fasciculus (IFOF2) or SLF. Since MD did not add further information about group differences, it was omitted in further analyses. Post hoc comparisons revealed significantly lower FA values for congenitally and late blind subjects bilaterally in ILF and posterior IFOF (IFOF1). This FA decrease was accompanied by a relative increase in radial diffusivity (Table 3), but without changes in axial diffusivity. An increase in radial diffusivity is compatible with the interpretation that the fibres are less densely packed and less aligned to each other in both groups of blind individuals. Supplementary Table 1 lists the FA and radial diffusivity values for all tracts. Neither subject age ($p = 0.194$) nor ROI size (Table 2) had a significant effect on the DTI indices, and were hence ignored in the ensuing analyses. We did not find any differences in white matter microstructure between preterm and at-term

sighted controls. Figure 3 shows that mean FA for all ROIs in preterm subjects is similar to those of normal sighted subjects, but differ significantly from those of both blind groups. To rule out purported effects due to age difference across groups, we performed an additional analysis, comparing a sub-sample of the normal sighted control subjects below the age of 40 years (mean age = 30 years) with the preterm subjects. This analysis failed to find significant differences in median FA between normal sighted controls and preterm subjects for any of the tract ROI (results not shown).

## Correlation with the blindness duration index

To assess the effects of the duration of visual experience on white matter microstructural changes in late blind individuals, we performed a correlation analysis with the blindness duration index (Table 1). We removed one outlier whose FA values were more than 2.7 SDs from the mean for all tracts. As illustrated in Fig. 4, there was a positive linear correlation between FA and BDI for the left ILF ($\beta = 0.554$, $p = 0.040$) and IFOF1 ($\beta = 0.638$, $p = 0.014$), indicating that the LB individuals who had been blind longer had higher FA values. The correlation between FA and BDI for the right ILF ($\beta = 0.334$, $p = 0.243$) and IFOF1 ($\beta = 0.492$, $p = 0.074$) did not reach significance level. Comparing FA values with the onset of blindness leads to a similar conclusion (Supplementary Figure 2).

Table 2 Between-group ANOVA of diffusion tensor indices in the tract ROIs

ROI	Source of variation (between group)	F value (left/right)	p value (left/right)
ILF	FA	16.970/10.367	<0.001/<0.001*
	RD	7.308/5.008	0.002*/0.012*
	AD	0.213/0.797	0.809/0.458
	ROI size	0.614/1.865	0.546/0.168
IFOF1	FA	11.085/10.937	<0.001*/<0.001*
	RD	5.395/3.490	0.001*/0.003*
	AD	1.491/1.020	0.238/0.370
	ROI size	0.694/1.859	0.505/0.169
IFOF2	FA	0.973/1.196	0.387/0.313
	RD	1.308/2.881	0.282/0.068
	AD	1.015/3.510	0.372/0.040
	ROI size	0.355/0.152	0.704/0.860
SLF	FA	1.579/2.058	0.129/0.141
	RD	3.091/2.936	0.057/0.065
	AD	4.189/2.184	0.022/0.126
	ROI size	0.853/1.865	0.434/0.168

ROI region of interest, *FA* fractional anisotropy, *RD and AD* radial and axial diffusivity, *ILF* inferior longitudinal fasciculus, *IFOF* inferior fronto-occipital fasciculus, 1 being the posterior part and 2 the anterior part, *SLF* superior longitudinal fasciculus

* $p < 0.01$ significant difference between groups
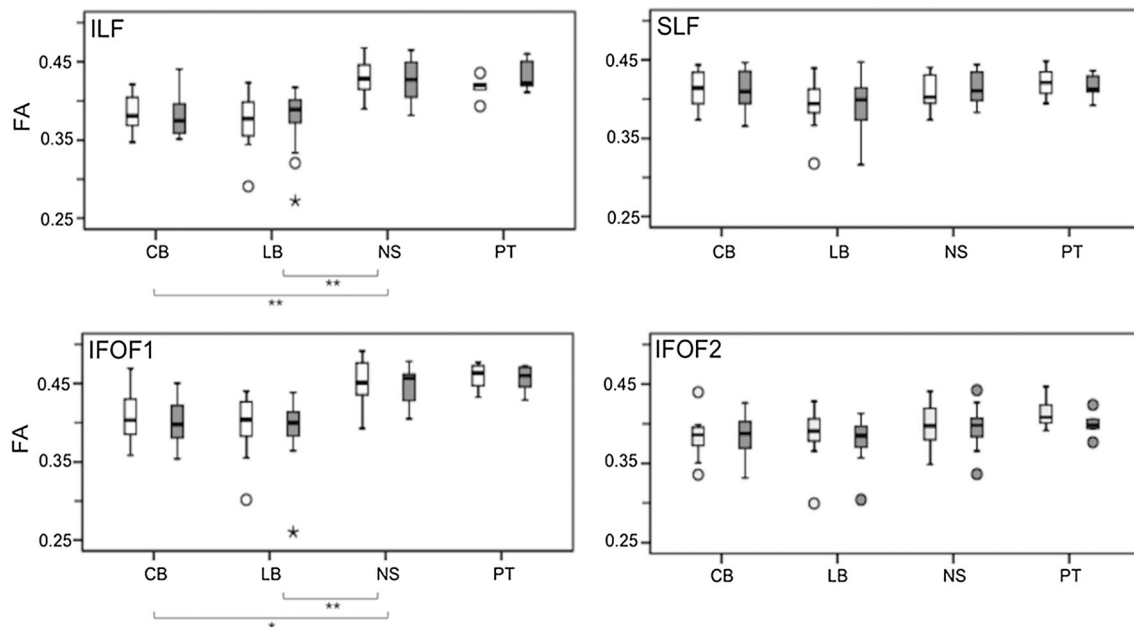
Fig. 3 Boxplots of the FA values for left (*open*) and right (*filled*) tract ROIs. The *black line* inside the *boxes* corresponds to the median value, the *box* edges the 25th and 75th percentiles, the whiskers the maximum and minimum values not considered as outliers. *Black circles* represent outliers and *asterisks* extreme values. Significant group differences between blind and sighted participants can be observed for the *left* and *right* ILF and IFOF1 (*$p < 0.005$; **$p < 0.001$). The FA values of normal sighted and preterm subjects were very similar. *NS* normal sighted, *CB* congenitally blind, *LB* late blind, *PT* preterm

Table 3 P values of the post hoc comparison of the microstructural features for ILF and IFOF1 in the congenitally (CB) and late (LB) blind group

ROI	FA, corrected p	RD, corrected p
ILF		
L	CB < NS: $p = 0.000$	CB > NS: $p = 0.053$
	LB < NS: $p = 0.000$	LB > NS: $p = 0.002$
R	CB < NS: $p = 0.003$	CB > NS: $p = 0.079$
	LB < NS: $p = 0.001$	LB > NS: $p = 0.012$
IFOF1		
L	CB < NS: $p = 0.004$	CB > NS: $p = 0.064$
	LB < NS: $p = 0.000$	LB > NS: $p = 0.001$
R	CB < NS: $p = 0.004$	CB > NS: $p = 0.129$
	LB < NS: $p = 0.000$	LB > NS: $p = 0.002$

p values are corrected for multiple comparisons, and considered significant at $p < 0.05$. Abbreviations as in Table 2

*L/R* left and right hemisphere

Discussion

In the present study, we showed that although the visual streams are structurally developing without normal visual input from the eyes, the microstructure of the ventral stream was affected by both congenital and late-onset visual loss, whereas the dorsal stream was unaffected by the loss of vision. The DTI indices revealed a decrease in mean FA in white matter tracts belonging to the ventral stream, driven by a relative increase in radial diffusivity, whereas we found no evidence for alterations in the dorsal stream. In the normally maturing white matter, a general increase in mean FA and a decrease in mean diffusivity have been suggested to reflect increased myelination, growth of axon calibre, and reduced free extra-cellular water (Paus 2010). The decreased FA in blind individuals might, therefore, relate to abnormalities in such white matter maturational processes. We have previously shown that decreased FA and increased radial diffusivity correlate negatively with a measure of axonal diameter (Alexander et al. 2010), and positively with axonal density. We, therefore, suggest that the here reported microstructural changes could indicate a reduction in fibre density in the ventral pathway in blind individuals. Even though the tractography-based complementary examination of tract volume and tract density did not reveal significant differences between blind and sighted individuals, we found a tendency towards a decreased tract density of the ILF in the blind compared to sighted controls when constraining the analysis to the core parts of the tracts. This observation supports the idea that increased radial diffusivity and decreased fractional anisotropy can reflect decreased axonal density. Importantly, tract density is an artificial measure that does not reflect the true axonal fibre density and that also cannot be directly related to the underlying

Fig. 4 Scatterplot with a linear curve fit between FA values and blindness duration index (*BDI*) for the ILF (*left panel*) and IFOF1 (*right panel*) in late blind individuals. A significant positive linear correlation was found for left ILF ($p = 0.040$) and left IFOF1 ($p = 0.014$) (*black lines*)
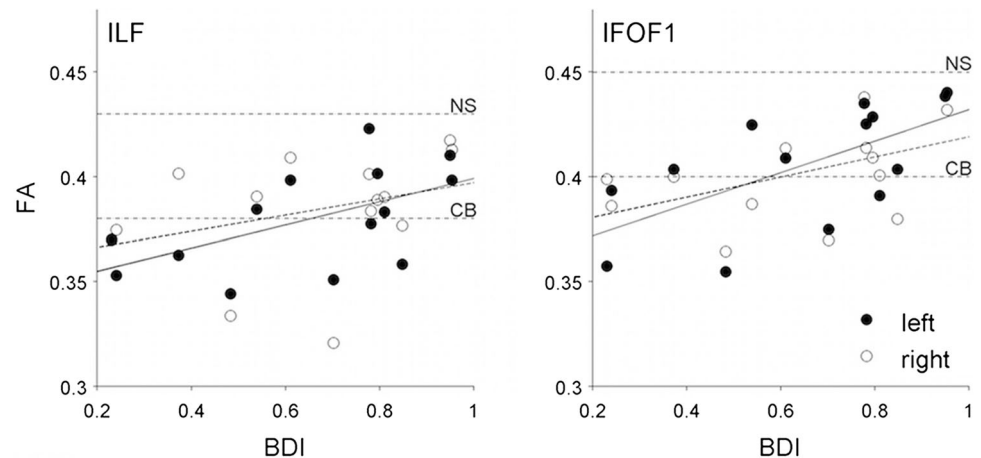
microstructural properties of the tissue. Our tract density measures should only be seen as supportive information to explain the observed microstructural differences.

Differential effects in the ventral and dorsal visual stream

One of the key findings of this study is that blindness affects the microstructural features of the ventral but not of the dorsal visual pathway. This finding is in line with those of Qin et al. (2013) who reported that in congenitally blind individuals, resting state functional connectivity is more affected among cortical areas belonging to the ventral as opposed to the dorsal stream. Previous functional brain imaging studies have shown that the basic functions of object recognition and spatial localisation are preserved in congenitally blind individuals through cross-modal plastic rearrangements (for review, see Kupers et al. 2011b). For example, Pietrini et al. (2004) reported activation of the ventral pathway in blind individuals when performing a tactile object recognition task, which resembled the activation pattern observed in sighted individuals when doing the same task visually. Similar findings have been reported for activation of the dorsal pathway, when visuo-spatial tasks were resolved using auditory or tactile inputs (Vanlierde et al. 2003; Ricciardi et al. 2007; Bonino et al. 2008; Matteau et al. 2010; Renier et al. 2010). Results of an fMRI study on kinaesthetic movement processing in congenitally blind and sighted control subjects further suggested that the dorsal pathway functions can develop independently of visual input (Fiehler et al. 2009). Hence, the dorsal stream system uses other sensory inputs to sustain the dorsal stream function, which might explain our findings of normal structural features of the dorsal stream in congenital and late blind individuals.

How to explain the differential effect of loss of vision on microstructural features of the ventral and dorsal streams?

One possibility is that this is due to important differences in the time course of the maturation of the ventral and dorsal visual streams in the human brain. Although the dorsal stream is functionally mature earlier than the ventral stream (Bourne 2010), white matter structural maturation is slower in the former (for review, see Lebel et al. 2008; Paus 2010; Klaver et al. 2011). Loenneker et al. (2011) compared maturation of the dorsal and ventral stream in 5–7 years old and 20–30 years old. The authors reported that age-related changes, including increased FA and decreased radial diffusivity along with an increase in tract volume, were much larger in the dorsal than in the ventral stream. This finding can be explained by the early structural maturation of the ventral pathway. As fibre tracts of the dorsal stream continue to mature until early adulthood, they have a much longer time-window during which cross-modal plastic processes can shape their maturation. On the contrary, the fibres of the ventral stream are already matured in childhood and thus do not allow the similar degree of plasticity, possibly explaining the selective decrease in FA in the ventral stream only.

An important related question is whether these microstructural alterations in the ventral visual pathways affect its functioning? Behavioural and functional neuroimaging studies have provided converging evidence that despite its changes in microstructural features, the ventral visual stream remains functionally active in blind individuals. Both behavioural and functional neuroimaging studies, using sensory substitution devices, consistently showed that congenitally blind subjects are able to perform a wide variety of high-order "visual" functions pertaining to both the dorsal and ventral streams (Kupers and Ptito 2013 for review). Together, this suggests that although visual loss causes microstructural alterations of the ventral stream, cross-modal plastic processes help to maintain its functional integrity (Amedi et al. 2002; Pietrini et al. 2004; Ricciardi et al. 2007; Renier et al. 2010; Kupers and Ptito 2013).

Congenital versus late-onset blindness

An unexpected finding was that we did not find DTI-based differences in the microstructural changes in white matter between congenitally and late blind subjects. Despite the difference in speed of the maturation of the two visual pathways, both groups showed similar white matter changes in the ventral stream relative to individuals with normal vision, and normal white matter features of the dorsal stream. Although the microstructural measures are similar in congenitally and late blind groups, their origin may be different. The positive linear correlation between the BDI and FA values of the ventral stream in our late blind participants indicates that individuals who become blind early in life show FA values more similar to those of normal sighted participants, whereas those who become blind later in life have FA values more resembling those of congenitally blind individuals. The change in FA value between early and late acquired blindness may be explained by the fact that in the former condition, the visual system is not yet fully developed at the time of onset of blindness, making it more susceptible to cross-modal plasticity. In case of late onset of blindness, the visual system has developed normally; instead of a plastic rearrangement, the fully matured tracts will undergo atrophic changes, explaining the drop in FA. Alternatively, certain fibre populations may become selectively destructed, whereas others may become enhanced over time, leading to a relative enhancement of the latter in the same voxel. A possible scenario could be that the major visual tracts become atrophic while smaller tracts and multiple connections with other sensory areas become strengthened with passage of time. The hypothesis of degenerative versus plastic changes in late and congenitally blind individuals, respectively, was also evoked to explain why a thicker visual cortex correlates with superior musical performance in CB, whereas a thinner visual cortex reflects atrophy in LB (Voss and Zatorre 2012). It has also been proposed that the plastic adjustment in late blind subjects might be dependent upon a "critical period" of brain development related to the onset of blindness (Cohen et al. 1999; Sadato et al. 2002; Burton 2003). An interesting question that still remains to be tested is whether the reported plastic adjustments in acquired blindness are reversible if vision can be restored.

Possible effects of preterm birth

A large portion of our congenitally blind participants has blindness due to retinopathy of prematurity. This syndrome is caused by oxygenation of preterm infants that may result in vasoconstriction of the retinal blood vessels, followed by an ischaemic insult. As preterm birth may lead to alterations in grey and white matter (Nosarti et al. 2008; Wan

et al. 2013), any purported findings in our congenitally blind subjects might be attributed to the fact that this group contained a high proportion of individuals who were born preterm. To rule out this possibility, we included a control group of preterm individuals with normal or corrected-to-normal vision. We did not find any significant white matter differences in the ventral or dorsal visual stream between preterm and at-term normal sighted individuals. The similar mean FA values in both groups suggest that the white matter changes in our congenitally blind cannot be attributed to preterm birth.

Methodological considerations

By adopting precise anatomical protocols for the fibre extraction, we ensured that the tract ROIs contained only the fibres of interest without spatial overlap from other fibre structures, for example from the primary visual system. By focusing on the DTI analysis within a well-defined ROI, we assume that the DTI indices mainly reflect the microstructural properties of the tract (Vos et al. 2012). One of the purported mechanisms underlying structural plasticity in the blind brain involves de novo connections to other cortical areas through the formation of novel connections between U-fibres and the main "fibre-tract-highways" (Laemle et al. 2006; Karlen et al. 2006). We here focused on the microstructural properties within the long association fibres of the visual streams, and have not included the short association fibres connecting adjacent gyri that do not project through the selected ROI.

The anatomical course of the SLF and its subcomponents has been described in several ways in the literature (Petrides and Pandya 1984; Makris et al. 2005; Bernal and Altman 2010; Thiebaut de Schotten et al. 2011a, b; Jang and Hong 2012). We chose to extract the SLF as a single fibre tract as the data did not allow a consistent separation into the 3 minor branches of the SLF. We ensured to obtain a robust and homogeneous tract ROI within the SLF for the microstructural assessment, but did not find significant group differences, nor tendencies towards, in microstructural features or streamline density of the SLF as a whole. We, therefore, do not expect that subdividing the SLF in its subcomponents would have given a different result. We extracted the IFOF in an anterior (IFOF2) and a posterior (IFOF1) segment, thereby obtaining two robust fibre tract areas across subjects. It remains a matter of debate whether the IFOF is truly one fibre tract, or rather two different tracts or subcomponents (Schmahmann et al. 2007). Martino et al. (2010) identified a superficial and dorsal IFOF subcomponent, and a deep and ventral subcomponent, each connecting different cortical areas. We observed lower FA values in IFOF2 than in IFOF1, which could originate from differences in anatomical structures within the IFOF. However,

we observed clear fanning effects of the streamlines from tractography for both IFOF1 and especially IFOF2. This fanning fibre effect also induced a larger inhomogeneity in the mean streamline density estimates of the IFOF in all groups. This suggests that the DTI results may be affected by unwanted fanning, bending, and spreading fibre effects (Descoteaux et al. 2009), and may explain the FA difference observed in IFOF1 and IFOF2. It also underlines the importance of always ensuring homogenous white matter ROIs as was done in this study when assessing the actual underlying microstructural properties to minimise contamination of such incoherent fibre effects.

Conflict of interest The authors declare that they have no conflict of interest.

References

Alexander DC, Hubbard PL, Hall MG et al (2010) Orientationally invariant indices of axon diameter and density from diffusion MRI. Neuroimage 52:1374–1389. doi:10.1016/j.neuroimage.2010.05.043

Amedi A, Malach R, Hendler T et al (2001) Visuo-haptic object-related activation in the ventral visual pathway. Nat Neurosci 4:324–330

Amedi A, Jacobson G, Hendler T et al (2002) Convergence of visual and tactile shape processing in the human lateral occipital complex. Cereb Cortex 12:1202–1212. doi:10.1093/cercor/12.11.1202

Basser PJ, Mattiello J, Lebihan D (1994) MR diffusion tensor spectroscopy and imaging. Biophys J 66:259–267

Bernal B, Altman N (2010) The connectivity of the superior longitudinal fasciculus: a tractography DTI study. Magn Reson Imaging 28:217–225. doi:10.1016/j.mri.2009.07.008

Bonino D, Ricciardi E, Sani L et al (2008) Tactile spatial working memory activates the dorsal extrastriate cortical pathway in congenitally blind individuals. Arch Ital Biol 146:133–146

Bourne JA (2010) Unravelling the development of the visual cortex: implications for plasticity and repair. J Anat 217:449–468. doi:10.1111/j.1469-7580.2010.01275.x

Bridge H, Cowey A, Ragge N, Watkins K (2009) Imaging studies in congenital anophthalmia reveal preservation of brain architecture in "visual" cortex. Brain 132:3467–3480. doi:10.1093/brain/awp279

Burton H (2003) Visual cortex activity in early and late blind people. J Neurosci 23:4005–4011

Catani M, Thiebaut de Schotten M (2008) A diffusion tensor imaging tractography atlas for virtual in vivo dissections. Cortex 44:1105–1132. doi:10.1016/j.cortex.2008.05.004

Catani M, Jones DK, Donato R, Ffytche DH (2003) Occipito-temporal connections in the human brain. Brain 126:2093–2107. doi:10.1093/brain/awg203

Clarke S (1994) Modular organization of human extrastriate visual cortex: evidence from cytochrome oxidase pattern in normal and macular degeneration cases. Eur J Neurosci 6:725–736

Cohen LG, Weeks RA, Sadato N et al (1999) Period of susceptibility for cross-modal plasticity in the blind. Ann Neurol 45:451–460

Collignon O, Dormal G, Albouy G et al (2013) Impact of blindness onset on the functional organization and the connectivity of the occipital cortex. Brain 136:2769–2783. doi:10.1093/brain/awt176

Descoteaux M, Deriche R, Knösche TR, Anwander A (2009) Deterministic and probabilistic tractography based on complex fibre orientation distributions. IEEE Trans Med Imaging 28:269–286. doi:10.1109/TMI.2008.2004424

Ffytche DH, Blom JD, Catani M (2010) Disorders of visual perception. J Neurol Neurosurg Psychiatry 81:1280–1287. doi:10.1136/jnnp.2008.171348

Fiehler K, Burke M, Bien S et al (2009) The human dorsal action control system develops in the absence of vision. Cereb Cortex 19:1–12. doi:10.1093/cercor/bhn067

Horton JC, Hedley-Whyte ET (1984) Mapping of cytochrome oxidase patches and ocular dominance columns in human visual cortex. Philos Trans R Soc Lond B Biol Sci 304:255–272. doi:10.2307/2396915

Jang SH, Hong JH (2012) The anatomical characteristics of superior longitudinal fasciculus I in human brain: diffusion tensor tractography study. Neurosci Lett 506:146–148. doi:10.1016/j.neulet.2011.10.069

Jellison BJ, Field AS, Medow J et al (2004) Diffusion tensor imaging of cerebral white matter: a pictorial review of physics, fiber tract anatomy, and tumor imaging patterns. AJNR Am J Neuroradiol 25:356–369

Jespersen SN, Lundell H, Sønderby CK, Dyrby TB (2013) Orientationally invariant metrics of apparent compartment eccentricity from double pulsed field gradient diffusion experiments. NMR Biomed 26:1647–1662. doi:10.1002/nbm.2999

Jespersen SN, Lundell H, Sønderby CK, Dyrby TB (2014) Commentary on "Microanisotropy imaging: quantification of microscopic diffusion anisotropy and orientation of order parameter by diffusion MRI with magic-angle spinning of the q-vector". Front Phys. doi:10.3389/fphy.2014.00028

Jeurissen B, Leemans A, Jones DK et al (2011) Probabilistic fiber tracking using the residual bootstrap with constrained spherical deconvolution. Hum Brain Mapp 32:461–479. doi:10.1002/hbm.21032

Jezzard P, Balaban RS (1995) Correction for geometric distortions in echo planar images from B0 field variations. Magn Reson Med 34:65–73

Jiang J, Zhu W, Shi F et al (2009) Thick visual cortex in the early blind. J Neurosci 29:2205–2211. doi:10.1523/JNEUROSCI.5451-08.2009

Karlen SJ, Kahn DM, Krubitzer L (2006) Early blindness results in abnormal corticocortical and thalamocortical connections. Neuroscience 142:843–858. doi:10.1016/j.neuroscience.2006.06.055

Klaver P, Marcar V, Martin E (2011) Neurodevelopment of the visual system in typically developing children. Prog Brain Res 189:113–136. doi:10.1016/B978-0-444-53884-0.00021-X

Kravitz DJ, Saleem KS, Baker CI, Mishkin M (2011) A new neural framework for visuospatial processing. Nat Rev Neurosci 12:217–230. doi:10.1038/nrn3008

Kravitz DJ, Saleem KS, Baker CI et al (2013) The ventral visual pathway: an expanded neural framework for the processing of object quality. Trends Cogn Sci 17:26–49

Kupers R, Ptito M (2011) Insights from darkness: what the study of blindness has taught us about brain structure and function. Prog Brain Res 192:17–31. doi:10.1016/B978-0-444-53355-5.00002-6

Kupers R, Ptito M (2013) Compensatory plasticity and cross-modal reorganization following early visual deprivation. Neurosci Biobehav Rev 13:191–207

Kupers R, Beaulieu-Lefebvre M, Schneider FC et al (2011a) Neural correlates of olfactory processing in congenital blindness. Neuropsychologia 49:2037–2044. doi:10.1016/j.neuropsychologia.2011.03.033

Kupers R, Pietrini P, Ricciardi E, Ptito M (2011b) The nature of consciousness in the visually deprived brain. Front Psychol. 2:1–14. doi:10.3389/fpsyg.2011.00019

Laemle LK, Strominger NL, Carpenter DO (2006) Cross-modal innervation of primary visual cortex by auditory fibers in congenitally anophthalmic mice. Neurosci Lett 396:108–112. doi:10.1016/j.neulet.2005.11.020

Lasič S, Szczepankiewicz F, Eriksson S et al (2014) Microanisotropy imaging: quantification of microscopic diffusion anisotropy and orientational order parameter by diffusion MRI with magic-angle spinning of the q-vector. Front Phys 2:1–14. doi:10.3389/fphy.2014.00011

Lawes INC, Barrick TR, Murugam V et al (2008) Atlas-based segmentation of white matter tracts of the human brain using diffusion tensor tractography and comparison with classical dissection. Neuroimage 39:62–79. doi:10.1016/j.neuroimage.2007.06.041

Lebel C, Walker L, Leemans A et al (2008) Microstructural maturation of the human brain from childhood to adulthood. Neuroimage 40:1044–1055. doi:10.1016/j.neuroimage.2007.12.053

Leemans A, Jeurissen B, Sijbers J, Jones DK (2009) ExploreDTI: a graphical toolbox for processing, analyzing, and visualizing diffusion MR data. International Society for Magnetic Resonance in Medicine, p 3537

Li J, Liu Y, Qin W et al (2013) Age of onset of blindness affects brain anatomical networks constructed using diffusion tensor tractography. Cereb Cortex 23:542–551. doi:10.1093/cercor/bhs034

Loenneker T, Klaver P, Bucher K et al (2011) Microstructural development: organizational differences of the fiber architecture between children and adults in dorsal and ventral visual streams. Hum Brain Mapp 32:935–946. doi:10.1002/hbm.21080

Makris N, Kennedy DN, McInerney S et al (2005) Segmentation of subcomponents within the superior longitudinal fascicle in humans: a quantitative, in vivo, DT-MRI study. Cereb Cortex 15:854–869. doi:10.1093/cercor/bhh186

Martino J, Brogna C, Robles SG et al (2010) Anatomic dissection of the inferior fronto-occipital fasciculus revisited in the lights of brain stimulation data. Cortex 46:691–699. doi:10.1016/j.cortex.2009.07.015

Matteau I, Kupers R, Ricciardi E et al (2010) Beyond visual, aural and haptic movement perception: hMT+ is activated by electrotactile motion stimulation of the tongue in sighted and in congenitally blind individuals. Brain Res Bull 82:264–270. doi:10.1016/j.brainresbull.2010.05.001

Noppeney U (2007) The effects of visual deprivation on functional and structural organization of the human brain. Neurosci Biobehav Rev 31:1169–1180. doi:10.1016/j.neubiorev.2007.04.012

Noppeney U, Friston KJ, Ashburner J et al (2005) Early visual deprivation induces structural plasticity in gray and white matter. Curr Biol 15:R488–R490. doi:10.1016/j.cub.2005.06.053

Nosarti C, Giouroukou E, Healy E et al (2008) Grey and white matter distribution in very preterm adolescents mediates neurodevelopmental outcome. Brain 131:205–217. doi:10.1093/brain/awm282

Park H-J, Lee JD, Kim EY et al (2009) Morphological alterations in the congenital blind based on the analysis of cortical thickness and surface area. Neuroimage 47:98–106. doi:10.1016/j.neuroimage.2009.03.076

Paus T (2010) Growth of white matter in the adolescent brain: myelin or axon? Brain Cogn 72:26–35. doi:10.1016/j.bandc.2009.06.002

Petrides M, Pandya DN (1984) Projections to the frontal cortex from the posterior parietal region in the rhesus monkey. J Comp Neurol 228:105–116. doi:10.1002/cne.902280110

Pietrini P, Furey ML, Ricciardi E et al (2004) Beyond sensory images: object-based representation in the human ventral pathway. Proc Natl Acad Sci USA 101:5658–5663. doi:10.1073/pnas.0400707101

Poirier C, Collignon O, Scheiber C et al (2006) Auditory motion perception activates visual motion areas in early blind subjects. Neuroimage 31:279–285. doi:10.1016/j.neuroimage.2005.11.036

Ptito M, Schneider FCG, Paulson OB, Kupers R (2008) Alterations of the visual pathways in congenital blindness. Exp Brain Res 187:41–49. doi:10.1007/s00221-008-1273-4

Ptito M, Matteau I, Gjedde A, Kupers R (2009) Recruitment of the middle temporal area by tactile motion in congenital blindness. NeuroReport 20:543–547. doi:10.1097/WNR.0b013e3283279909

Ptito M, Matteau I, Zhi Wang A et al (2012) Crossmodal recruitment of the ventral visual stream in congenital blindness. Neural Plast. doi:10.1155/2012/304045

Qin W, Liu Y, Jiang T, Yu C (2013) The development of visual areas depends differently on visual experience. PLoS ONE 8:e53784. doi:10.1371/journal.pone.0053784

Reese TG, Heid O, Weisskoff RM, Wedeen VJ (2003) Reduction of eddy-current-induced distortion in diffusion MRI using a twice-refocused spin echo. Magn Reson Med 49:177–182. doi:10.1002/mrm.10308

Renier LA, Anurova I, De Volder AG et al (2009) Multisensory integration of sounds and vibrotactile stimuli in processing streams for "What" and "Where". J Neurosci 29:10950–10960. doi:10.1523/JNEUROSCI.0910-09.2009

Renier LA, Anurova I, De Volder AG et al (2010) Preserved functional specialization for spatial processing in the middle occipital gyrus of the early blind. Neuron 68:138–148. doi:10.1016/j.neuron.2010.09.021

Ricciardi E, Vanello N, Sani L et al (2007) The effect of visual experience on the development of functional architecture in hMT+. Cereb Cortex 17:2933–2939. doi:10.1093/cercor/bhm018

Sadato N, Okada T, Honda M, Yonekura Y (2002) Critical period for cross-modal plasticity in blind humans: a functional MRI study. Neuroimage 16:389–400. doi:10.1006/nimg.2002.1111

Schmahmann JD, Pandya DN, Wang R et al (2007) Association fibre pathways of the brain: parallel observations from diffusion spectrum imaging and autoradiography. Brain 130:630–653. doi:10.1093/brain/awl359

Schoth F, Burgel U, Dorsch R et al (2006) Diffusion tensor imaging in acquired blind humans. Neurosci Lett 398:178–182. doi:10.1016/j.neulet.2005.12.088

Shimony JS, Burton H, Epstein AA et al (2006) Diffusion tensor imaging reveals white matter reorganization in early blind humans. Cereb Cortex 16:1653–1661. doi:10.1093/cercor/bhj102

Shu N, Li J, Li K et al (2009) Abnormal diffusion of cerebral white matter in early blindness. Hum Brain Mapp 30:220–227. doi:10.1002/hbm.20507

Strnad L, Peelen MV, Bedny M, Caramazza A (2013) Multivoxel pattern analysis reveals auditory motion information in MT+ of both congenitally blind and sighted individuals. PLoS ONE 8:e63198

Thiebaut de Schotten M, Dell'Acqua F, Forkel SJ et al (2011a) A lateralized brain network for visuospatial attention. Nat Neurosci 14:1245–1246. doi:10.1038/nn.2905

Thiebaut De Schotten M, Dominic H, Bizzi A et al (2011b) Atlasing location, asymmetry and inter-subject variability of white matter tracts in the human brain with MR diffusion tractography. Neuroimage 54:49–59. doi:10.1016/j.neuroimage.2010.07.055

Tournier J-D, Mori S, Leemans A (2011) Diffusion tensor imaging and beyond. Magn Reson Med 65:1532–1556. doi:10.1002/mrm.22924

Ungerleider LG, Mishkin M (1982) Two cortical visual systems. In: Ingle DJ, Goodale M, Mansfield RJW (eds) Analysis of visual behaviour, pp 549–586

Vanlierde A, De Volder AG, Wanet-Defalque M-C, Veraart C (2003) Occipito-parietal cortex activation during visuo-spatial imagery in early blind humans. Neuroimage 19:698–709. doi:10.1016/S1053-8119(03)00153-8

Vos SB, Jones DK, Viergever MA, Leemans A (2011) Partial volume effect as a hidden covariate in DTI analyses. Neuroimage 55:1566–1576. doi:10.1016/j.neuroimage.2011.01.048

Vos SB, Jones DK, Jeurissen B et al (2012) The influence of complex white matter architecture on the mean diffusivity in diffusion tensor MRI of the human brain. Neuroimage 59:2208–2216. doi:10.1016/j.neuroimage.2011.09.086

Voss P, Zatorre RJ (2012) Occipital cortical thickness predicts performance on pitch and musical tasks in blind individuals. Cereb Cortex 22:2455–2465. doi:10.1093/cercor/bhr311

Wakana S, Jiang H, Nagae-poetscher LM, et al (2003) Radiology fiber tract based Atlas of radiology, pp 21–29

Wakana S, Caprihan A, Panzenboeck MM et al (2007) Reproducibility of quantitative tractography methods applied to cerebral white matter. Neuroimage 36:630–644. doi:10.1016/j.neuroimage.2007.02.049

Wan CY, Wood AG, Chen J et al (2013) The influence of preterm birth on structural alterations of the vision-deprived brain. Cortex 49:1100–1109. doi:10.1016/j.cortex.2012.03.013

Westin C-F, Maier SE, Mamata H et al (2002) Processing and visualization for diffusion tensor MRI. Med Image Anal 6:93–108

Wheeler-Kingshott CAM, Cercignani M (2009) About "axial" and "radial" diffusivities. Magn Reson Med 61:1255–1260. doi:10.1002/mrm.21965

Yu C, Shu N, Li J et al (2007) Plasticity of the corticospinal tract in early blindness revealed by quantitative analysis of fractional anisotropy based on diffusion tensor tractography. Neuroimage 36:411–417. doi:10.1016/j.neuroimage.2007.03.003

Zhang H, Hubbard PL, Parker GJM, Alexander DC (2011) Axon diameter mapping in the presence of orientation dispersion with diffusion MRI. Neuroimage 56:1301–1315. doi:10.1016/j.neuroimage.2011.01.084